

CAD-Enhanced Workspace Optimization for Parallel Manipulators: A Case Study

Hrishi Shah, Madusudanan Sathia Narayanan and Venkat N. Krovi, *Member, IEEE*

Abstract—The challenges of workspace determination of parallel manipulators (PMs) arise principally from the lack of analytical solutions of the forward kinematics. The inverse-position kinematics based approach for determining workspace tends to be inefficient, time consuming and unsophisticated. In this paper, we present a geometry-based method for accurate and computationally effective calculation of the workspace of a constrained parallel manipulator. We illustrate how boolean geometric operations can simplify the process of finding the workspace and optimizing the designs. Comparative performance studies, in terms of accuracy and computational performance, are performed to benchmark the approach against more conventional methods. Finally, we examine ways to further automate the process using a CAD package.

I. INTRODUCTION

Parallel-architecture robotic-manipulators offer numerous advantages, in terms of increased stiffness and higher load-carrying capacities [1], making them attractive for numerous applications. However, the creation and deployment of new parallel-architecture robotic-manipulators face challenges mainly due to the presence of closed-kinematic loops ranging from workspace-design to control-analysis and ultimately the final implementation.

This paper focuses on the workspace-design aspect for such parallel-architecture manipulators – with the primary goal of optimizing the link geometries and parameters to enhance overall workspace and other selected geometric workspace-based performance-measures. In particular, we will focus on the aspect that a parallel manipulator's workspace can be determined as the intersection of the individual serial-supporting chains i.e. by geometric union and/or intersection of supporting serial-chain workspace volumes.

Two facets contribute to the increased computation cost and complexity of this approach to workspace analysis. First, while the process is conceptually simple and trivially

implemented for planar manipulators, the complexity increases considerably for spatial manipulators. Further, effective visualization is a key to workspace-design and analysis and is difficult for 6-DOF workspaces. Various types of workspaces have been studied in the literature [2], out of which two types are considered important: (i) a constant orientation workspace – the set of points which the manipulator can reach while keeping its orientation fixed; (ii) a constant position workspace – the set of orientations possible for the manipulator while keeping the position of the platform center fixed [3]. Automated methods for workspace maximization of parallel manipulators require effective workspace “performance measure” calculations to develop the objective functions. Hence, we evaluate applicability of workspace analysis using geometric programming techniques such as geometric constraint analysis and boolean operations on solid volumes.

The rest of the paper is organized as follows: In Section 2, some of the previous literature related to workspace-analysis and design optimization for parallel mechanisms are examined. In Section 3, the two exemplary parallel-architecture systems: (i) the Stewart-Gough (SG) 6-U-P-S (six passive-universal actuated prismatic and passive-spherical legs) parallel manipulator; and (ii) a specialized 6-P-U-S (six actuated-prismatic - passive-universal - passive-spherical legs) parallel manipulator are introduced. In Section 4, the proposed geometry-based workspace calculation techniques are discussed and then efficiency and performance of this improvised method against the conventional (parametric sweeping) method was evaluated. Finally, this scheme was extended to reap the benefits of automatic volume calculation and subsequent design-optimization using a parametric CAD tool. While our focus is the 6-P-U-S manipulator, the method is benchmarked comparing against published results for the SG platform.

II. BACKGROUND

Many researchers have studied workspace determination of 6-DOF parallel platform manipulators. Some early attempts like Saxena *et al.* [4] developed the constant orientation workspace using the parameter sweep method while Bonev and Gosselin [5] proposed the geometric approach to handling workspaces of parallel manipulators for a 6-R-U-S mechanism. While examining the constant orientation workspace of 6-DOF parallel has remained an actively researched topic, few of these studies have focused

Manuscript received March 12, 2010. This work was supported in part by the National Science Foundation Award CNS-0751132.

H. L. Shah is a M.S. student, with the Dept. of Mechanical & Aerospace Engg, State University of New York at Buffalo, Buffalo, NY 14260, USA (email: hshah@buffalo.edu)

M. S. Narayanan is a Ph. D. student, with the Dept. of Mechanical & Aerospace Engg, State University of New York at Buffalo, Buffalo, NY 14260 USA (email: ms329@buffalo.edu)

V. N. Krovi is an Associate Professor with the Dept. of Mechanical & Aerospace Engg, State University of New York at Buffalo, 318 Jarvis Hall, Buffalo, NY 14260, USA (Ph: 716 645 1430, F: 716 645 3668, email: vkrovi@buffalo.edu).

on symbolic solution process and its automation. An attempt was made [6] to find a singularity free orientation workspaces (previously referred to as constant position workspace) of the Stewart platform. Merlet *et al.* [7], were able to find various subsets of the orientation workspace. Using geometric methods to solve for the constant position workspace is an ongoing research area and is not covered in this paper.

Tanaka *et al.*[8], attempted to use the intersection of multiple spheres describing the feasible movements of all the different serial manipulators. However, the work remained limited to the visualization case and no efforts at quantization (workspace volumes and optimization) were pursued. A similar intersection-workspace visualization concept was used [9] for a spatial 6-PRRS using CATIA script-programming. In contrast, in this paper, we seek to use the CAD package to both (i) characterize various aspects of the workspace using quantitative-measures; as well as (ii) use workspace performance-measures for optimization to achieve another level of automation in a mechanism design process.

III. EXAMPLE SYSTEMS

A. Stewart-Gough (SG) Parallel Manipulator

The Stewart-Gough platform is a classic example of a 6-DOF parallel platform manipulator that consists of a platform attached to a base through six articulated legs [10]. Each articulated leg is of a Universal-Prismatic-Spherical (U-P-S) architecture- controlling the six leg-lengths simultaneously (via the active prismatic joints) allows control of platform pose. Such an SG platform shown in Figure 1, will serve as a benchmark against which we validate our workspace optimization framework.



Figure 1: Typical Stewart Platform Depiction

B. 6-P-U-S Parallel Manipulator

However, our primary interest is to apply this workspace optimization framework to enhance the workspace of a 6-P-U-S parallel manipulator, whose kinematic study was reported in [11-12]. This parallel manipulator consists of six legs, each having a P-U-S architecture as shown in Figure 2 and Figure 3. Each pair of legs has collinear prismatic joints and shares a common distal spherical joint – they can be combined into a single subsystem, which will be referred to as Two-Link-Subsystem (TLS) as depicted in Figure 4. Such an architecture, with common connection points on the platform, simplifies the kinematics considerably. Further, the active prismatic joints are located on the ground, thereby effectively reducing the weight of the connecting links (as

compared to legs of Stewart platform) and making the manipulator more energy efficient [13].

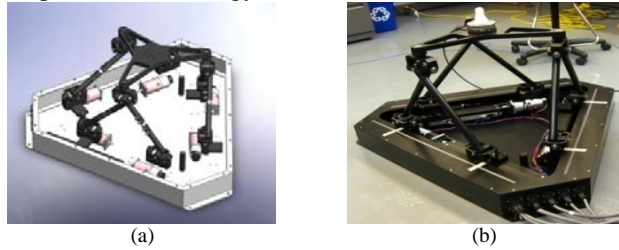


Figure 2: 6-P-U-S with 6 Actuated Prismatic Joints Located at the Base: (a) CAD Model (b) Physical Prototype

IV. DETAILED FORMULATION

The reference-frames for 6-P-U-S manipulator are aligned as shown in Figure 3. The inertial reference-frame is attached at the centroid (O) of the equilateral triangle formed by the base prismatic joints. The local reference-frames are at the centers of the three sides of this equilateral triangle. The end-effector (EE) reference frame is attached at the centroid (P) of the equilateral triangle formed by the central platform.

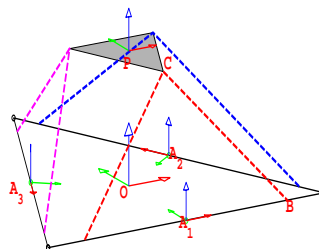


Figure 3: Reference Frames for 6-P-U-S Manipulator

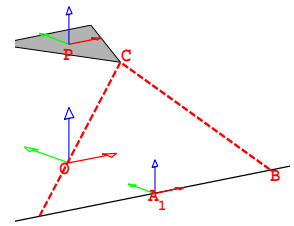


Figure 4: Two-Link Subsystem (TLS) for 6-P-U-S

In Figure 3, the solid (black) line represents the line of action of the base prismatic joints, which for all the six prismatic joints combined form an equilateral triangle with its center at the origin (O). The measurements of slider positions are carried out from the centers of the sides of this triangle (A_i), where the reference frames are located. The thick dotted lines (red, blue and magenta) represent the links connected to the base prismatic sliders (B_i) via universal joints at the proximal-end and by distal-spherical joints (C_i) to the central platform (shaded in gray), whose center is at P.

We now focus on finding the constant-orientation workspace for this mechanism in the nominal home pose ($[\alpha, \beta, \gamma]^T = [0, 0, 0]^T$) and simplifying the process using geometric methods. The transformations between the various frames can be developed as:

$${}^{A_i}T^O = \begin{bmatrix} \cos(\alpha_i) & -\sin(\alpha_i) & 0 & bx_i \\ \sin(\alpha_i) & \cos(\alpha_i) & 0 & by_i \\ 0 & 0 & 1 & bz_i \\ 0 & 0 & 0 & 1 \end{bmatrix} \quad (1)$$

where, α_i is the angle of the X-axis of the i^{th} TLS' prismatic joints with the X-axis of the inertial reference frame, and (bx_i, by_i, bz_i) are the coordinates of the origin of the i^{th} TLS expressed in global coordinates. Hence, given the side length

rewritten as:

$$\overline{OP} = \overline{OA} + \overline{AB} + \overline{BC} - \overline{PC} \quad (4)$$

Similar equations for other TLSs can be written by equating \overline{OP} :

$$\overline{OA_1} + \overline{A_1B_1} + \overline{B_1C_1} - \overline{PC_1} = \overline{OA_2} + \overline{A_2B_2} + \overline{B_2C_2} - \overline{PC_2} \quad (5)$$

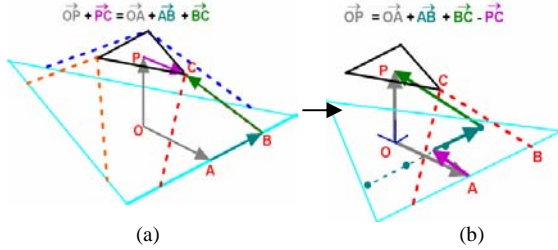


Figure 7: Method C- Exact Workspace Using Geometric Constraints

As can be seen, all the vectors except $\overline{B_1C_1}$ and $\overline{B_2C_2}$ are known and can be substituted for in (5). The magnitude of the unknown vectors is also known (link lengths, L). Hence, we can reduce the problem of finding the end-effector position to a problem of intersecting spheres. This is illustrated graphically in Figure 7, which shows original loop closure in (2) and the modified relation in (5).

In Figure 7, the dots on the line parallel to a prismatic joint axis through A_i represent the slider limits. Hence, we note that the link is at the maximum displacement of the right prismatic joint. Hence, the workspace can now be calculated by cycling through the range of prismatic motions. We notice here that in order for any point to lie along the workspace boundaries, at least one of the prismatic joints must have reached their motion limits. Hence, any surface in the entire workspace should lie along one of the limit spheres with a prismatic limit point as its center and the link length as its radius. Similarly, any edge of the workspace (intersection of two spherical surfaces) would be along the intersection of two spheres such that limit constraints on any two prismatic sliders are active simultaneously. Similarly, any intersection point of the workspace (intersection of two curves) would be the intersection of three spheres, or at those points, the limit constraints for three sliders are simultaneously active.

To find the workspace, we start with the intersection points between different spherical surfaces. We note that there are totally 12 limit points for the 6 prismatic joints. Considering that any prismatic joint can only be at one of the two limits at the same instant, we eliminate two of the 12 initially available limit points by assuming one prismatic joint at its limit. Thus, we find the total number of 3-sphere intersection points by finding the total number of combinations which is,

$$n = (12) * (12-2) * (12-2-2) = 960 \quad (6)$$

Next, we find the actual intersection points for all of these possibilities and check whether they satisfy conditions for other links to reach the point in consideration (whether the other 3 links assumed not to be at the limits are feasibly

placed to reach this point using (3)). This criterion is similar to the previous method that decreases the number of points from 960 to the actual number of points on the workspace (18 in this particular example) that we need to find. The last step is to find the points with two common spheres and draw

TABLE 2: METHOD COMPARISON (ACCURACY)

	Method A (for different grid sizes)			Method C	Difference
	0.1 (a)	0.05 (b)	0.025 (c)	Exact (d)	(d-b)
Min X	-0.800	-0.850	-0.850	-0.875	-0.025
Min Y	-0.900	-0.900	-0.900	-0.918	-0.018
Min Z	1.400	1.400	1.350	1.333	-0.017
Max X	0.800	0.800	0.800	0.797	-0.004
Max Y	0.700	0.750	0.750	0.775	0.025
Max Z	2.400	2.400	2.400	2.420	0.020

curves between them along their intersection.

Finally, we find the curves having a common sphere index and plot the surfaces between them along the common sphere. The resulting workspace envelope obtained is plotted in Figure 8 and Figure 9. To verify the validity of this approach, we eliminate the surface plots from Method C and overlay the resulting line plot with the workspace plot from Method A as shown in Figure 9. As expected, the workspace envelope obtained by Method C is similar to, though more accurate than the one obtained from the parameter sweep method A. Furthermore, it can also be verified that the differences are less than the grid size used in Method A (0.05 in this case) as shown in Table 2. We also see that as the grid size decreases, the min/max X/Y/Z values from Method A converge to those found by using Method C. Figure 10 compares the volume computed by the Method A (solid line) and B (dotted line) with varying mesh sizes using the CAD model volume obtained by Method D. We observe the variation between the CAD model and volumes obtained by Method A and Method B. The errors typically are of the order of 0.1 % until the grid size reaches 0.07 with the volume calculations from Methods A and B matching exactly.

Now, in order to perform a comparative study between the different methods, we use the common computing platform with the following specifications—Pentium Dual-Core 2.1Ghz Processor with 4GB RAM and Windows 7 Home Premium. The corresponding CPU times required to complete the workspace computation are documented in Table 4. The times noted here are based from unoptimized MATLAB codes (running in the interpreted mode) and are intended to be indicative of type of speedups across the methods.

We observe that employing Method B saves almost 96% of the time as compared to Method A. There is a further improvement of around 17% in computation time when switching from Method B to Method C. Another disadvantage of parameter sweeps is that in the absence of proper initial guesses for the cube to encompass the workspace, some regions of the workspace might have been ignored or additional design space might be searched, both of which are undesired for optimal workspace computation.

Hence, we note that using a geometry-based approach for parallel manipulators can be more efficient as well as accurate.

D. Using CAD modeling software to compute volumes

Finally, we note that the above three approaches relied on the user's ability to code part of the computation in MATLAB. Alternately, a 3D CAD package (commercial or open source software) could be used to compute the volume

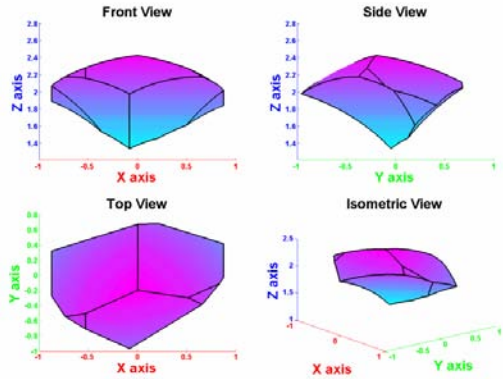


Figure 8: Method C - 3D Workspace

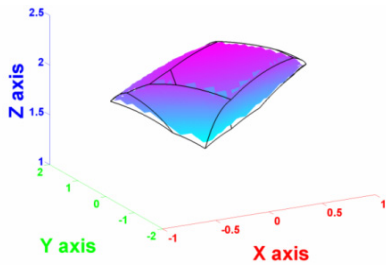


Figure 9: Comparison of Calculated Workspace based on Method A (Solid Line) v/s Method C (Shaded Region)

TABLE 3: PARAMETER SWEEP VALUES FOR CAD MODEL

Parameter	Axis	Min	Max	Resolution	# Values
L_A -Platform Length	X	1.0	3.0	0.1	21
R_1 - Link Length	Y	2.3	4.3	0.1	21
Volume	Z	0.4	1.26	-	441

of intersection of the feasible regions of all three TLS. We also note that the CAD package is being used to compute the intersection of the spheres and not to perform the 3D detailed drawing of the parallel manipulator in question.

1) 6-P-U-S Parallel Manipulator

In this method, we input the known geometric parameters for the hexapod – L (side of base equilateral triangle), l (side of central platform) as well as the platform's constant orientation as $[\alpha, \beta, \gamma]^T$ – the Euler angles representing the XYZ rotation of the central plate. Using Method C with this, we can create spheres with centers at the limit points (as in Figure 7) and radii equal to leg-lengths. The volume trapped between two spheres corresponding to the two limits of a single prismatic joint represents the possible location of the end-point achievable by that leg. The same procedure is repeated for the other five legs. An intersection of these six volumes provides the overall workspace. The resulting workspace obtained from Pro-E matched closely with that of

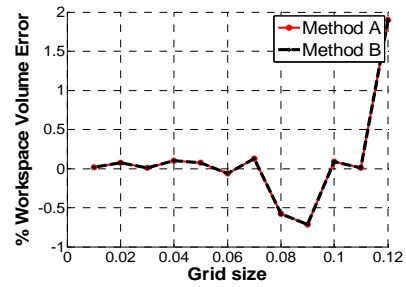


Figure 10: Percentage Volume Error (Method A and B w.r.t. Method D v/s Grid Size)

TABLE 4: METHODS COMPARISON (CPU TIMES)

Method	CPU Time (s)	Improvement w.r.t Method A (%)
Method A(0.05)	29.241(total)/ 20.373(computation)	0
Method B (0.05)	0.878(total/computation)	95.69
Method C (exact)	0.731(total/computation)	16.74 (Met. B) 96.41 (Met. A)

the MATLAB results as shown in Figure 9. To validate and generalize this method, we examined the workspace for another constant orientation of the end effector— $[30, 20, 0]^T$. The 3D workspace obtained using methods B and D for this case are found to be nearly same as in Figure 11.

The added advantages of using a CAD software is that it allows easy calculation of the various workspace parameters like volume (which is difficult using MATLAB codes as in Methods A, B and C) and easier design-optimization formulation within its package. For example, the volume of the constant orientation workspace for zero orientation can be found as 0.717 unit^3 while the same for $[30, 20, 0]^T$ is given by 0.126 unit^3 . In addition, if the links were made of length equal to 2.5 units, the volume for zero orientation would be 0.964 unit^3 . This could imply that having different link-lengths for hexapod would greatly inhibit its workspace and hence, it would be best to keep all links of equal length. Further, we could also analyze how changing this equal length could change the workspace. For instance, changing this equal link length to 2.7 units changes the workspace volume to $.842 \text{ unit}^3$.

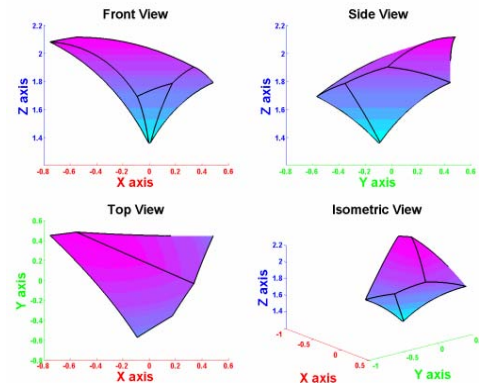


Figure 11: Workspace Obtained by Method C - $([\alpha, \beta, \gamma]^T = [30, 20, 0]^T)$

To find the computation effectiveness of this approach, we programmed in ProE for a parameter sweep to find the volume of the workspace. The program required

approximately 42.5 seconds for a test run of 441 points (details shown in Table 3). The results of this sweep were exported to a csv file and plotted using MATLAB as in Figure 12. Further, optimization studies may be setup (using a feature available within parametric CAD packages) to maximize/minimize the workspace volume. In this instance, we made a case for maximum workspace volume with the central platform length and the link lengths as the parameters. One physical use of such a study would be to find the maximum possible workspace achievable with a given space limitation for a machine.

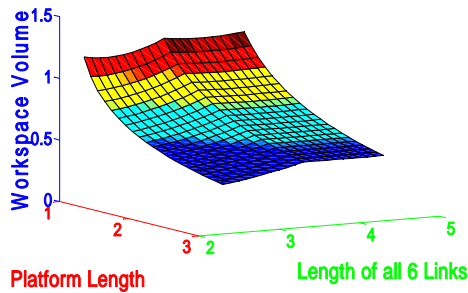


Figure 12: Parameter Sweep from CAD System

TABLE 5: WORKSPACE OPTIMIZATION IN PRO-E

Parameter	Before Optimization	After Optimization
Workspace Volume	0.717 units ³	1.264 units ³
Central platform length	1.5 units	1.809 units
TLS1 Link length	2.5 units	2.256 units
TLS2 Link length	2.7 units	2.255 units
TLS3 Link length	2.6 units	2.250 units

Results of a sample optimization study are shown in Table 5. As can be seen, all the optimized leg lengths are nearly equal. This observation for various parameter values for central platform length and axis angles led to a conclusion that keeping all the leg lengths equal would result in the maximum possible workspace volume formed by varying the link lengths. Many such conclusions can be drawn depending on the variables being altered and this may aid in better mechanism design.

2) Stewart-Gough Platform (Benchmark Problem)

This method can be applied to the Stewart Platform with minor changes to the CAD model. Only the equations (2)-(5) and the local reference frame locations need to be modified for \bar{CP} to resemble the Stewart platform. Thus, its workspace can be easily obtained. Figure 13 visually

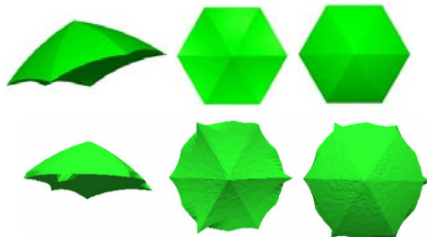


Figure 13: Comparison of Our Results (top-row) against the Published Benchmark (bottom row) [8]

compares the results for the zero-orientation workspace, obtained using the parameters from [8].

V. DISCUSSION/CONCLUSION

In this paper, we examined an alternate and flexible method of workspace evaluation using CAD modeling software. We note that such geometric programming methods (constraint analysis and boolean volumetric operations) could potentially be much more insightful, efficient and accurate than conventional parameter sweep methods and illustrated this with an example. Finally, we compared and benchmarked this method against published results for a known parallel-architecture manipulator – allowing us to demonstrate significant potential for workspace design-refinement.

VI. REFERENCES

- [1] J. P. Merlet, *Parallel Robots (Solid Mechanics and Its Applications)*, 2nd ed.: Springer, February 2006.
- [2] F. Pernkopf and M. L. Husty, "Workspace Classification of Stewart—Gough Manipulators with Planar Base and Platform," in *On Advances in Robot Kinematics*, J. Lenarcic and C. Galletti, Eds., ed Sestri Levanta, Italy, 2004, pp. 229-238.
- [3] I. A. Bonev and C. M. Gosselin, "A Geometric Algorithm for the Computation of the Constant-Orientation Workspace of 6- \underline{R} U S Parallel Manipulators," in *Proceedings of the ASME Design Engineering and Technical Conference (DETC 2000)*, Baltimore, MD, September 10-13, 2000.
- [4] V. Saxena, D. Liu, and C. M. Daniel, "A Simulation Study of the Workspace and Dexterity of a Stewart Platform Based Machine Tool," in *Proc. 1997 ASME International Mechanical Engineering Congress and Exposition*, Dallas, TX, USA, November 16 - 21, 1997.
- [5] I. A. Bonev and C. M. Gosselin, "Geometric Algorithms for the Computation of the Constant-Orientation Workspace and Singularity Surfaces of a special 6- \underline{R} U S Parallel Manipulator," in *Proc. ASME Design Engineering Technical Conferences (DETC 2002)*, Montreal, Quebec, Canada, September 29 – October 2, 2002.
- [6] Q. Jiang and C. M. Gosselin, "Evaluation and Representation of the Theoretical Orientation Workspace of the Gough-Stewart Platform," *Journal of Mechanisms and Robotics*, vol. 1, p. 9, 2009.
- [7] J. P. Merlet, "Determination of 6D Workspaces of Gough-Type Parallel Manipulator and Comparison Between Different Geometries," *International Journal of Robotics Research*, vol. 18, pp. 902-916, 1999.
- [8] Y. Tanaka, I. Yokomichi, J. Ishii, and M. Wakiyama, "Evaluation of Workspace in Parallel Machines," in *Proc. International Conference on Advances in Construction Machinery and Vehicle Engineering*, 2007.
- [9] I. A. Bonev and J. Ryu, "Workspace Analysis of 6-PRRS Parallel Manipulators Based on the Vertex Space Concept," in *Proc. ASME Design Engineering Technical Conferences (DETC 1999)*, Las Vegas, NV, September 12-15, 1999.
- [10] L.-W. Tsai, *Robot Analysis: The Mechanics of Serial and Parallel Manipulators*. New York, N.Y.: John Wiley & Sons, 1999.
- [11] M. S. Narayanan, "Analysis of Parallel Platform Architectures for Use in Masticatory Studies," M.S. Thesis, Mechanical and Aerospace Engineering, University at Buffalo (SUNY), Buffalo, NY, 2008.
- [12] M. S. Narayanan, H. L. Shah, and V. N. Krovi, "Kinematic-, Static- and Workspace Analysis of a 6- \underline{P} U S Parallel Manipulator," in *Proc. ASME Design Engineering Technical Conferences (DETC 2010)*, Montreal, Quebec, Canada, Aug 15-18, 2010.
- [13] I. A. Bonev, "Geometric Analysis of Parallel Mechanisms," Ph. D. Dissertation, Laval University, Canada, Quebec, Nov 2002.
- [14] Y. Lou, G. Liu, N. Chen, and Z. Li, "Randomized Optimal Design of Parallel Manipulators," *IEEE Transactions on Automation Science and Engineering*, vol. 5, pp. 223-233, April 2008.
- [15] A. M. Hay, "Optimal Dimensional Synthesis of Planar Parallel Manipulators with Respect to Workspaces," Ph. D. Dissertation, Mechanical Engineering, University of Pretoria, Pretoria, October 2003.